

Linear instability of turbulent channel flow

Pavan V. Kashyap,¹ Yohann Duguet,¹ and Olivier Dauchot²

¹LIMSI-CNRS, UPR 3251, Université Paris-Saclay, 91405 Orsay, France

²Gulliver Lab, UMR CNRS 7083, ESPCI Paris, PSL University, 75005 Paris, France

(Dated: May 12th, 2022)

Laminar-turbulent pattern formation is a distinctive feature of the intermittency regime in subcritical plane shear flows. Performing extensive numerical simulations of the plane channel flow, we show that the pattern emerges from a spatial modulation of the turbulent flow, due to a linear instability. We sample over many realizations, the linear response of the fluctuating turbulent field to a temporal impulse, in the regime where the turbulent flow is stable, just before the onset of the instability. The dispersion relation is constructed from the ensemble-averaged relaxation rates. As the instability threshold is approached, the relaxation rate of the least damped modes eventually reaches zero. The method allows, despite the presence of turbulent fluctuations and without any closure model, for an accurate estimation of the wavevector of the modulation at onset.

Turbulent channel flow is one of the most studied prototypes of inhomogeneous anisotropic turbulence. It has been evidenced, both experimentally and numerically, that at moderate flow rates – as quantified by the Reynolds number Re – it exhibits a spatio-temporally intermittent regime featuring robust large-scale turbulent structures amid a laminar background [1–3]. The dynamical origin of such patterned turbulence in channel flow, as well as in other shear flows such as plane Couette flow (pCf) [4–6] and Taylor-Couette flow (TCf) [5–8], remains however actively debated.

On the lower end in Re of the coexistence regime, turbulent patches grow and split, or decay, resulting in strongly fluctuating dynamics. It was suggested that the stochastic nature of these processes, which decides whether turbulence will either spread or recede and eventually decay, could be described in the framework of non-equilibrium critical phenomena and specifically of directed percolation (DP), with the laminar state acting as the absorbing phase [9]. A major achievement of the past two decades has been to provide strong experimental and numerical evidences in favour of this scenario in a few shear flows [10–12]. On the theoretical side, this regime has been described by an effective one-dimensional model of fronts in an excitable medium [13, 14]. Quite remarkably, and yet not theoretically understood, numerical simulations of the stochastic version of the model reproduce the DP scenario.

Increasing Re , individual turbulent patches leave place to a coexistence organized at the flow scale [7, 8], in the form of a well organized periodic pattern of alternating laminar and turbulent bands, inclined at a well defined angle to the mean flow [5]. Considering the proliferation of turbulence as a problem of front propagation, it is tempting to view this pattern as packed arrays of individual localized structures. Yet, periodic pattern solutions have not been identified as solutions to the effective

excitable dynamics [13, 14]. An alternative viewpoint is to consider the pattern as emerging from the featureless turbulence found at larger Re . Pioneering studies have demonstrated experimentally that the pattern developing in pCf and TCf, which is characterised by two competing orientation of alternate sign, is fully captured by the dynamics of two coupled Ginburg-Landau equations with noise [5, 6]. Recent visualizations, obtained in well-resolved numerical simulations of large domains channel flows unveil small-amplitude harmonic modulations of the turbulent flow for values of Re larger than those at which genuine laminar-turbulent coexistence is reported [3]. Statistical signatures of low-wall-shear-rate intermittency have been found, at Re -values usually associated with featureless turbulent flows [15]. Altogether these results suggest the possibility of a large-wavelength instability of the *turbulent flow* itself, as already proposed in [5]. As recently suggested on the basis of a spatiotemporal extension of a classical self-sustained turbulence model [16, 17], the instability could be of Turing type [18]. However, there is no theoretical evidence for such a linear instability of the turbulent mean flow obtained from one-point closure models [19]. These different viewpoints reflect global doubts regarding the origins of the patterned state and ambiguity as to whether the starting point for modeling the periodic pattern should be the spatial organization of the isolated turbulent patches when increasing Re , or the linear instability of the turbulent flow, including its fluctuations, when decreasing Re .

Here we bring direct evidence in favour of the linear instability scenario in the case of the channel flow. To do so, we perform extensive numerical simulations and sample the linear response of the turbulent flow to a temporal impulse, in the regime where the large wavelength modulations are damped. The dispersion relation is then constructed from the ensemble-averaged re-

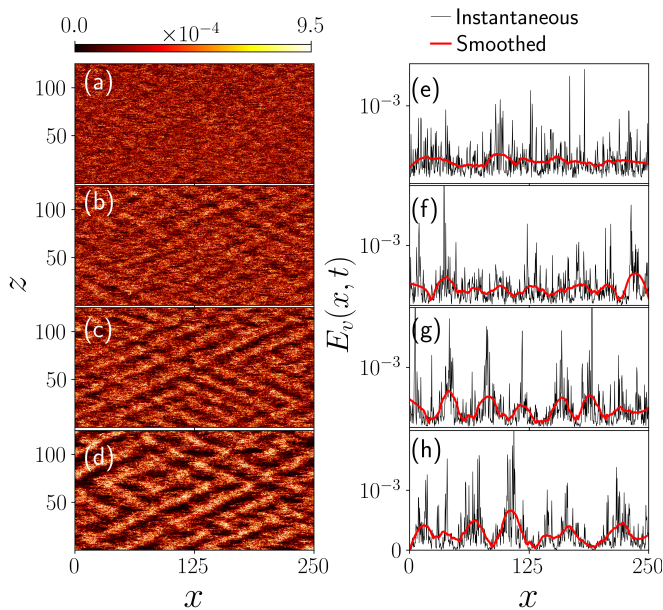


FIG. 1. Onset of modulated turbulent channel flow. Left column: turbulent kinetic energy $E_v(x, z)$; right column: instantaneous streamwise profile of $E_v(x, z = cst)$, (black: raw instantaneous values, red: low-pass filtered values). From top to bottom : (a,b) $Re_\tau = 100$, (c,d) $Re_\tau = 90$, (e,f) $Re_\tau = 85$, (g,h) $Re_\tau = 80$.

laxation rates, for decreasing values of Re . The smallest relaxation rate approaches zero, eventually becomes positive, for some critical value Re_c , pointing at the spatial structure of the modes which grow at the instability onset. The method can be seen as the temporal counterpart of the spatial linear response considered in [20]. It is intrinsically statistical in the sense that it establishes an *average dispersion relation* for the instability modes, from which the quantitative onset for the spatial modulation can be identified.

The incompressible flow considered in this study is driven in the streamwise direction x by a constant pressure gradient. The other Cartesian coordinates y and z are respectively wall-normal and spanwise. The selected control parameter is the friction Reynolds number $Re_\tau = u_\tau h / \nu$, where h is the half-gap between the two walls, ν is the kinematic viscosity of the fluid, $u_\tau = \sqrt{\tau} / \rho$ is the friction velocity, with τ the mean shear rate fixed by the pressure gradient, and ρ the fluid density. An alternative Reynolds number is $Re_{cl} = Re_\tau^2 / 2$, based on the centerline velocity of the classical laminar plane Poiseuille flow $U(y) = 1 - y^2$ driven by the same pressure gradient, which loses its stability at $Re_{cl} = 5772$. Turbulent simulations were performed with the spectral solver Channelflow2.0 [21] in a domain of $L_x = 2L_z = 250$ for times up to $t = 4,000$. These simulations are well resolved with a resolution of $N_x = N_z = 1024$ (including dealiasing with the 2/3 rule) comparable to [3]. The most recent investigations have reported laminar-turbulent patterns for $50 \lesssim Re_\tau \lesssim 90$, and independent turbulent bands for

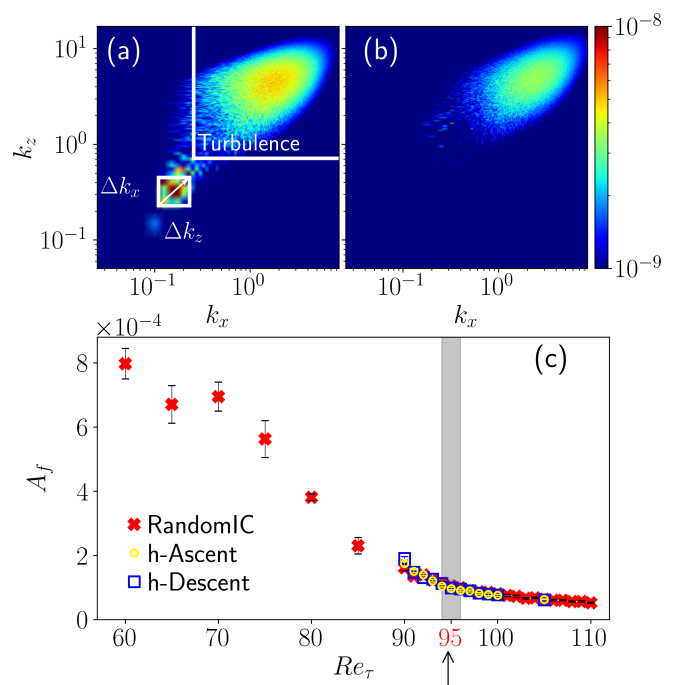


FIG. 2. (a) Premultiplied power spectrum for the y -averaged streamwise velocity fluctuation $\langle u'_x \rangle_y$ at $Re_\tau = 92$ (left) and $Re_\tau = 110$ (right). (b) Amplitude A_{LSF} of the large-scale modes (as defined in Eq. 2), vs. Re_τ (red cross : random initial conditions, blue square : descending annealing, yellow circle : ascending annealing). The black arrow points at the linear instability threshold corresponding to the onset of the turbulent modulated flow determined here at $Re_\tau = 95 \pm 1$.

lower values of Re_τ down to ≈ 36 [3, 15, 22, 23].

Large-scale modulations close to $Re_\tau \approx 90$, as well as genuine laminar-turbulent patterning for $Re_\tau \lesssim 90$, are unambiguous from Fig. 1, which displays the instantaneous turbulent kinetic energy

$$E_v(x, z) = \frac{1}{2} \int_{-1}^{+1} u_y^2 dy, \quad (1)$$

both at full spatial resolution and after application of a low-pass filter. It was checked that the modulations and the pattern are robust with respect to the doubling and quadrupling of the numerical domain in both x and z . The exact range of existence of the modulations, and notably their onset, are difficult to judge from visualizations alone because of the turbulent fluctuations, whose standard deviation can exceed the amplitude of the modulation. It is also sensitive to the choice of the visualized quantity. The emergence of large-scale patterns, as Re_τ decreases, appears however clearly as a low-wavenumber signature in the time-averaged two-dimensional energy spectrum of the y -averaged fluctuating component $\langle u'_x \rangle_y$ of the streamwise velocity (Figure 2-a). Apart from the small-scale modes, corresponding to the turbulent fluctuations, one clearly observes a

set of large-scale modes excited at $Re_\tau = 92$ but absent at $Re_\tau = 110$. These large-scale modes are also separated from the turbulent ones. Exploiting this scale separation, we define $A_{LSF}(Re_\tau)$, the amplitude of the large-scale flow, as the energy content of the spectral subdomain $\mathcal{S}_{LSF} = \{0.025 \lesssim k_x \lesssim 0.5, 0.05 \lesssim k_z \lesssim 0.8\}$, which is largely dominated by the low k excitation inside the square of area $\Delta k_x \Delta k_z$ highlighted in Fig. 2-a(left) :

$$A_{LSF}(Re_\tau) = \left(\frac{1}{\Delta k_x \Delta k_z} \int \bar{E}(k_x, k_z) dk_x dk_z \right)^{1/2}, \quad (2)$$

where $\bar{E}(k_x, k_z)$ is the time-averaged power spectrum. A_{LSF} is shown as a function of Re_τ in Fig. 2-b as obtained from random initial conditions or during slow ascent, respectively descent, annealing in Re_τ . One observes a clear increase of A_{LSF} as Re_τ decreases from the featureless turbulent regime ($Re_\tau \gtrsim 110$) to the well-defined pattern one ($50 \lesssim Re_\tau \lesssim 90$), with no sign of hysteresis. The transition between both regimes is however a smooth crossover rather than a sharp transition : A_{LSF} is never strictly zero, even in the featureless turbulent regime, owing to the turbulent fluctuations.

Establishing the linear instability of a flow with arbitrary time-dependence can be addressed in different ways. One possibility is to study the linear stability of the *mean* flow using the Orr-Sommerfeld formalism. This strategy whether conducted at high [24] or transitional [25] Re , concludes to linear stability. At the opposite end, taking into account all temporal fluctuations at once is in principle possible using Lyapunov analysis. However for turbulent flows the number of positive Lyapunov exponents is known to be prohibitively huge [26] because of the chaoticity at small scales down to the Kolmogorov scale. The turbulent scales where these instabilities dominate are however *not* the emerging large-scales visible in Fig. 2, leaving us with a tractable way out.

The general idea is to study the linear response of the flow to a temporal impulse. If the flow is linearly stable, the disturbance should relax, otherwise it should grow and lead to a bifurcated flow. However, the reference flow being turbulent, the analysis must be conducted at a statistical level. Also the spatial structure of the temporal impulse should be agnostic to the turbulent spectrum. We therefore proceed as follows. A representative turbulent state in the statistically steady regime at the required value of Re_τ , simulated for $t < 0$, is perturbed at $t = 0$ using a divergence-free *noise field*, before the simulations runs further without noise, for $t > 0$, and we monitor the temporal evolution of the modulus of the Fourier amplitudes of *large-scale modes*, $A_f(Re_\tau, k_x, k_z, t)$, with $(k_x, k_z) \in \mathcal{S} = \{0.075 \lesssim k_x \lesssim 0.22, 0.2 \lesssim k_z \lesssim 0.5\}$ (highlighted square area in Fig. 2-a). For large enough Re , the disturbed flow relaxes back towards the steady turbulent state. The individual time series $A_f(t)$ however

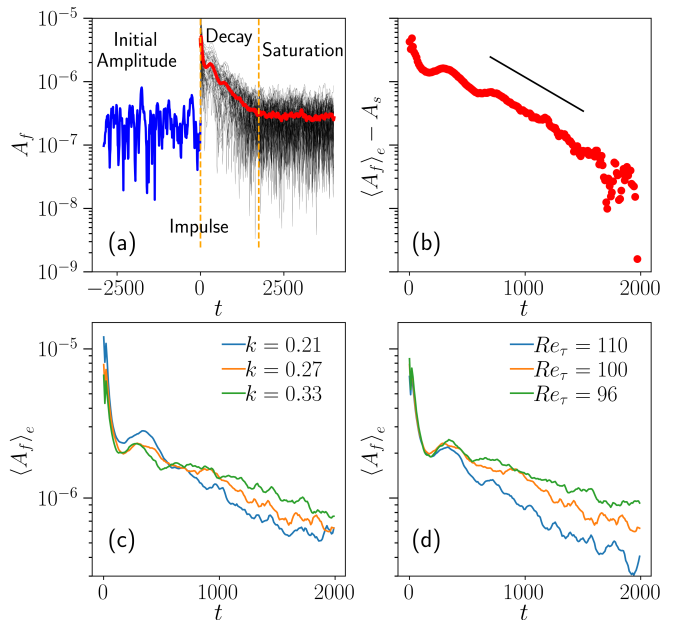


FIG. 3. (a) Temporal evolution of the amplitude of the Fourier mode $A_f(Re_\tau, k_x, k_z, t)$ with $(k_x, k_z) = (0.12, 0.3)$, ($k = 0.32$) and $Re_\tau = 120$; blue ($t < 0$), black: individual realizations for $t > 0$ and red: ensemble average $\langle A_f \rangle(t)$. (b) $\langle A_f \rangle(t) - A_s$, same (k_x, k_z) , same Re_τ , black: exponential fit. (c) $\langle A_f \rangle(t)$ for three different values of k , $Re_\tau = 100$. (d) $\langle A_f \rangle(t)$ for three different values of Re_τ , $k = 0.27$.

showcase noisy, non-exponential decay. This computational decay experiment is therefore repeated over 40 different realizations of the noise field and the modulus of the spectral amplitude of each large-scale Fourier mode is ensemble-averaged over all realizations as illustrated in figure 3-a for $Re_\tau = 120$ and $(k_x, k_z) = (0.12, 0.3)$. Ensemble-averaging brings clarity into the system's response: past an initially nonlinear decrease of $\langle A_f \rangle$, a clear exponential decay towards a finite value A_s is observed. This exponential decay captures the *averaged linear response* of the turbulent state with respect to a temporal impulse. The corresponding growth rate σ is evaluated by estimating first the saturation level A_s and then fitting an exponential decay to $(\langle A_f \rangle - A_s)$, using a straight line fit in logarithmic scale, as portrayed in figure 3-b. As a first step, the analysis is carried out along the diagonal of the spectral window \mathcal{S} . Fig. 3-c,d show the strong dependence of the growth rate on both $k = \sqrt{k_x^2 + k_z^2}$ and Re_τ . More specifically, one observes that, for $Re_\tau = 96$, the growth rate of the mode corresponding to $k = 0.38$ is close to vanishing, suggesting the proximity of a linear instability. In principle one could expect monitoring the average exponential growth of such a large-scale mode beyond the instability threshold. However the growth rate would be hard to measure accurately near onset. Besides one would need isolating

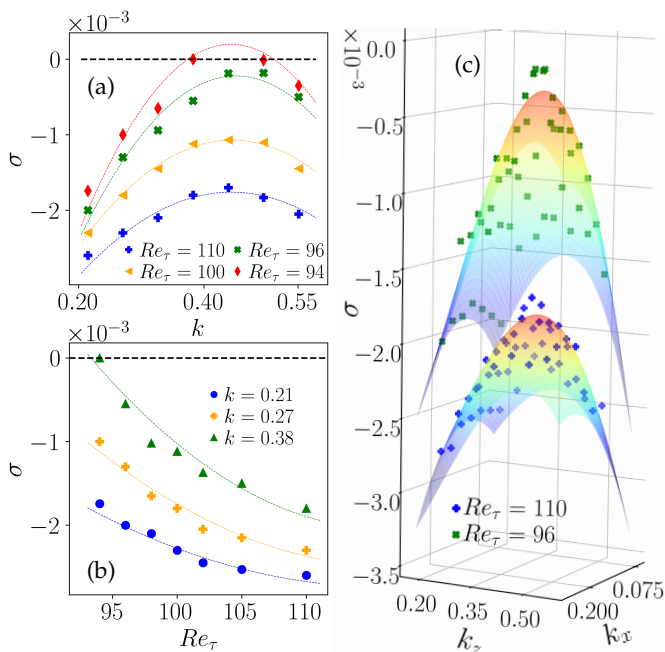


FIG. 4. Dispersion relation: (a) growth rate σ versus the streamwise wavenumber k_x parametrized by Re_τ (b) σ versus Re_τ parametrized by the wavenumber modulus $k = \sqrt{k_x^2 + k_z^2}$ (c) growth rate σ versus both k_x and k_z for two values of $Re_\tau = 96$ and 110. In both (a) and (b), the parabola are fitted to data, whereas in (c) the continuous line are only guides to the eye.

the featureless turbulent state in a regime where it is unstable.

We therefore concentrate on the decay rates and extract the mean dispersion relation for the linear response of the turbulent flow (Fig. 4). The dispersion curves approach the neutral axis as the value of Re_τ is decreased and eventually cross it for $Re_\tau = 94$. The estimated critical value for the instability is $Re_\tau = 95 \pm 1$. The critical wavevector ($k_x = 0.17 \pm 0.025$, $k_z = 0.4 \pm 0.05$) are obtained from a parabolic fit of the decay rates, estimated for all $(k_x, k_z) \in \mathcal{S}$, as illustrated in Fig. 4-c for $Re_\tau = 110$ and $Re_\tau = 96$. It perfectly matches the one measured directly at onset and lead to an inclination of the pattern with the streamwise direction of $23 \pm 0.5^\circ$, consistently with the measurements reported in [15]

This quantitative agreement validates the proposed methodology, i.e. the statistical analysis of the temporal impulse response, can be considered as a new experimental/numerical method to address the linear stability analysis of a steady, but fluctuating dynamics. Let us emphasize once again that the base flow considered here is the turbulent flow itself including all fluctuations [27], not the mean flow.

Altogether our results provide direct evidence for a lin-

ear instability of the turbulent state itself as first conjectured in [5]. This linear instability leads to a spatial modulation of the turbulent flow, the amplitude of which grows and saturates according to weakly nonlinear contributions [6]. For low enough Re_τ , the modulation breaks into a pattern of alternated turbulent and laminar bands. Further decreasing Re_τ these bands gain in independence and a proper stochastic front dynamics sets in.

Our work paves the way for future works in two main directions. First, one would like to identify the instability mechanism. A possible candidate, commonly encountered across diverse noisy chemical and biological systems [28] relies on the Turing instability [18, 29]. It is based on the competition between an inhibitor and an activator field with different diffusivities [30]. However this approach requires modelling of the turbulent diffusivity using e.g. simple first-moment closures [31]. Another possible approach is to consider a generalised stability analysis taking into account higher-order moments of the fluctuations [32]. Both approaches are based on closure assumptions. The instability unveiled in the present work represents an ideal and simple case to test these assumptions. The second future direction of research consists in identifying the strongly nonlinear scenario along which the pattern loses its spatial coherence. It remains a formidable challenge.

This study was made possible using computational resources from IDRIS (Institut du Développement et des Ressources en Informatique Scientifique) and the support of its staff. The developing team of `channelflow.ch` is also gratefully thanked. The authors also acknowledge constructive discussions with D. Barkley, L.S. Tuckerman and P. Manneville.

-
- [1] T. Tsukahara, Y. Seki, H. Kawamura, and D. Tochio (Begel House Inc., 2005), iSSN: 2642-0554.
 - [2] S. Hashimoto, A. Hasobe, T. Tsukahara, Y. Kawaguchi, and H. Kawamura, in *Turbulence Heat and Mass Transfer 6. Proceedings of the Sixth International Symposium On Turbulence Heat and Mass Transfer* (Begel House Inc., 2009).
 - [3] M. Shimizu and P. Manneville, *Physical Review Fluids* **4**, 113903 (2019), ISSN 2469-990X, arXiv: 1808.06479.
 - [4] Y. Duguet, P. Schlatter, and D. S. Henningson, *Journal of Fluid Mechanics* **650**, 119 (2010), ISSN 0022-1120, 1469-7645.
 - [5] A. Prigent, G. Grégoire, H. Chaté, O. Dauchot, and W. van Saarloos, *Physical Review Letters* **89**, 014501 (2002), ISSN 0031-9007, 1079-7114.
 - [6] A. Prigent, G. Grégoire, H. Chaté, and O. Dauchot, *Physica D: Nonlinear Phenomena* **174**, 100 (2003), ISSN 01672789.
 - [7] D. Coles, *Journal of Fluid Mechanics* **21**, 385 (1965), ISSN 1469-7645, 0022-1120, publisher: Cambridge University Press.

- [8] C. V. Atta, *Journal of Fluid Mechanics* **25**, 495 (1966), ISSN 1469-7645, 0022-1120, publisher: Cambridge University Press.
- [9] Y. Pomeau, *Physica D: Nonlinear Phenomena* **23**, 3 (1986), ISSN 01672789.
- [10] G. Lemoult, L. Shi, K. Avila, S. V. Jalikop, M. Avila, and B. Hof, *Nature Physics* **12**, 254 (2016), ISSN 1745-2473, 1745-2481.
- [11] M. Chantry, L. S. Tuckerman, and D. Barkley, *Journal of Fluid Mechanics* **824**, R1 (2017), ISSN 0022-1120, 1469-7645.
- [12] L. Klotz, G. Lemoult, K. Avila, and B. Hof, *Physical Review Letters* **128**, 014502 (2022), publisher: American Physical Society.
- [13] D. Barkley, *Physical Review E* **84**, 016309 (2011), ISSN 1539-3755, 1550-2376, arXiv: 1101.4125.
- [14] D. Barkley, *Journal of Physics: Conference Series* **318**, 032001 (2011), ISSN 1742-6596.
- [15] P. V. Kashyap, Y. Duguet, and O. Dauchot, *Entropy* **22**, 1001 (2020), number: 9 Publisher: Multidisciplinary Digital Publishing Institute.
- [16] F. Waleffe, *Physics of Fluids* **9**, 883 (1997).
- [17] O. Dauchot and N. Vioujard, *The European Physical Journal B-Condensed Matter and Complex Systems* **14**, 377 (2000).
- [18] P. Manneville, *EPL (Europhysics Letters)* **98**, 64001 (2012).
- [19] L. S. Tuckerman, D. Barkley, and O. Dauchot, in *Seventh IUTAM Symposium on Laminar-Turbulent Transition* (Springer Netherlands, Dordrecht, 2010), vol. 18, pp. 59–66, ISBN 978-90-481-3722-0 978-90-481-3723-7.
- [20] S. Russo and P. Luchini, *Journal of Fluid Mechanics* **790**, 104 (2016).
- [21] J. Gibson, F. Reetz, S. Azimi, A. Ferraro, T. Kreilos, H. Schrobdsdorff, N. Farano, A. F. Yesil, S. S. Schütz, M. Culpo, et al., manuscript in preparation (2022).
- [22] B. Song and X. Xiao, *Journal of Fluid Mechanics* **903** (2020), ISSN 0022-1120, 1469-7645, publisher: Cambridge University Press.
- [23] V. Mukund, C. Paranjape, M. P. Sitte, and B. Hof, arXiv preprint arXiv:2112.06537 (2021).
- [24] W. Reynolds and W. Tiederman, *Journal of Fluid Mechanics* **27**, 253 (1967).
- [25] L. S. Tuckerman, D. Barkley, and O. Dauchot, (private communication) (2010).
- [26] L. Keefe, P. Moin, and J. Kim, *Journal of Fluid Mechanics* **242**, 1 (1992).
- [27] A. S. Iyer, F. D. Witherden, S. I. Chernyshenko, and P. E. Vincent, *Journal of Fluid Mechanics* **875**, 758 (2019), ISSN 0022-1120, 1469-7645.
- [28] M. Cross and H. Greenside, *Pattern Formation and Dynamics in Nonequilibrium* (Cambridge University Press, Cambridge, 2009), ISBN 978-0-521-77050-7.
- [29] P. Kashyap, Ph.D. thesis, Université Paris-Saclay (2021).
- [30] A. M. Turing, *Philosophical Transactions of the Royal Society of London. Series B, Biological Sciences* **237**, 37 (1952), ISSN 0080-4622, publisher: The Royal Society.
- [31] J. C. Del Alamo and J. Jimenez, *Journal of Fluid Mechanics* **559**, 205 (2006).
- [32] V. K. Markeviciute and R. R. Kerswell, arXiv preprint arXiv:2201.01540 (2022).